CLIC Telescope Optimization with ALLPIX Simulation

2015 Summer Student Final Report

WU Qi (Supervisor: Mathieu Benoit)

Physics Department

Hong Kong University of Science and Technology (HKUST)

Clear Water Bay, Kowloon, Hong Kong, China

qi.wu@cern.ch

qwuad@ust.hk

I. Introduction

A. *Vertex Detector and EUDET*

The vertex detector, made of pixels, allows to measure the position of charged particles with high precision. The resolution of pixel detector therefore largely depends on the pitch size, sensor technology and ASICs. A telescope is used to determine the resolution of a new detector. It consists of several reference detecting chips whose performances are well known to reconstruct precisely the tracks. During the test beams for the CLIC vertex detector, the EUDET telescope is used which consists of 6 planes of MIMOSA 26 pixel sensors wish a tracking resolution of about $3\mu m$ for 5.6 GeV electron beam. The device under test (DUT) is placed between 3rd and the 4th layers (Fig. 1).

The tracks reconstructed by the EUDET telescope are extrapolated on the DUT in order to study the tracking efficiency of the tested device and determine its position resolution by calculating $\overrightarrow{x_{Telescope}} - \overrightarrow{x_{DUT}}$.

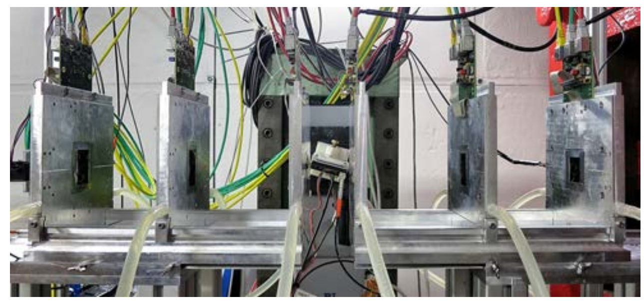

Fig. 1. CLIC-EUDET telescope setup[1].

B. *MIMOSA 26 Sensor and Silicon Tracker*

The MIMOSA 26 sensor is the first large scale sensor from the MIMOSA[2] series [1], to profit fully from the advantage of CMOS low mass pixel sensors, i.e. high granularity and thin sensitive volume, with read-out micro-circuits integrated on the sensing element. Same as all the other monolithic silicon sensors, MIMOSA 26 takes the advantage of the ionization effect to detect passing charged particles. When a high energy particle

[1] Picture Modified from Geneva Telescope Judith Website. https://twiki.cern.ch/twiki/bin/viewauth/GeneveAtlas/GenevaJudith

[2] Standing for Minimum Ionizing MOS Active pixel sensor

passes through the silicon detector, it deposits some energy to create thousands or tens of thousands of electron-hole pairs. By imposing a very high electronic voltage across the sensing element, electrons and hold would be moved toward opposite direction to two different specially-doped conductive regions, which are usually connected to electronics to create tiny currents and therefore called "contact". By amplification, one could detect the pulse and finally digitize them into raw data [2].

C. Simulation and Reconstruction Chain

The tracking resolution of the telescope depends on the beam energy and the position of the telescope planes in the space. With simulations, we could discuss and minimize the effects of these factors without wasting budgets to do too much actual experiments.

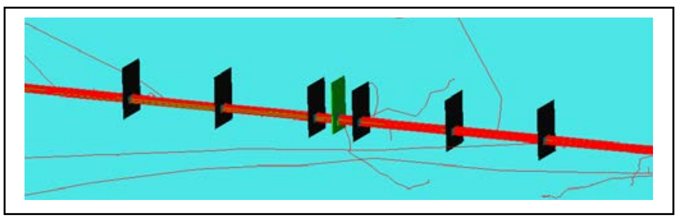

Fig. 2. Allpix simulation visualization.

In our project we used a software called ALLPIX[3] (Fig. 2) to produce simulation data with GEANT4[4]. ALLPIX saves every single event an ASCII file and one could convert the data into binary ".slcio" used by the linear collider community. After simulation, we could use one of the two software, EUTelescope[5] + pyEudetAnalysis[6] or Judith[7] [3] to analyze those data and stores results into ROOT files. The basic steps for analyzing data are similar: aligning, cluster searching, hits making and fitting. In aligning, one recursively adjusts the geometric position of each chips according to the firing distributions all the chip planes. By moving and rotating the planes, the difference between the firing distributions of different planes would be minimized to avoid the artificial effects produced by the actual imperfect experimental setting. Since in simulations, all the planes are perfectly aligned, the processes of alignment should usually be neglected. In cluster searching and hits making, one groups the firing pixel in terms of clusters and predicts the hitting position within each cluster by some algorithms, e.g. ***QWeighted*** and ***DigitalCentroid***. In fitting step, the tracks are reconstructed based on the hit position on the telescope planes and extrapolated to the DUT. In our project, we mainly used

[3] Software developed by John Idarraga idarraga@cern.ch Mathieu Benoit mbenoit@cern.ch Samir Arfaoui sarfaoui@cern.ch. Twiki site: https://twiki.cern.ch/twiki/bin/view/Main/AllPix

[4] A toolkit for the simulation of the passage of particles through matter. Software website: http://geant4.cern.ch/

[5] A Generic Pixel Telescope Data Analysis Framework. Software website: http://eutelescope.web.cern.ch/

[6] Python framework for analysis of EUDET telescope reconstructed data. Official GIT site: https://github.com/pyEudetAnalysis/pyEudetAnalysis

[7] Analysis software developed by University of Geneva ATLAS group. Official site: https://twiki.cern.ch/twiki/bin/viewauth/GeneveAtlas/GenevaJudith

EUTelescope + pyEudetAnalysis method to analyze the simulation data.

II. SIMULATION SETUPS

D. New Digitizer

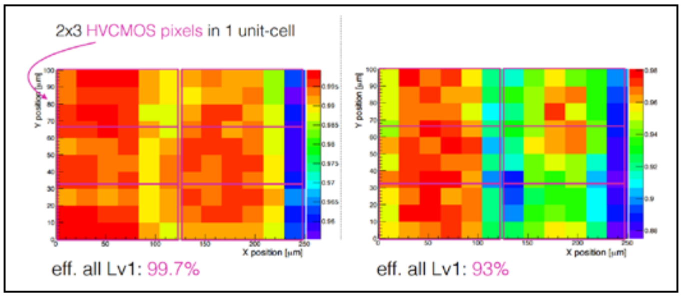

Fig. 3. Bad Cell efficiency maps: left) C19, unIrradiated Bias 90 V, Th 0.94 V; right) C22, 10^{15} n_{eq}/cm^2, Bias 80 V, Th 0.94 V. See reference for details [4].

In practice, any small defect on the pixel sensor come from the embedded electronics would greatly affect its overall efficiency (Bad example: Fig. 3, Good example: Fig. 4). It therefore requires high resolution telescopes in order to examine the existence and influences of these defects before using them. In our simulation, a special virtual detector, called "QiWu" in Allpix/qiwu-dev branch is defined which accepts the energy deposited onto each pixel only within a cylinder. By varying the radius of the cylinder and see the deformation of hit probability, we could be able to calculate the minimal resolution of the telescope. In our simulation, we compared the case with the cylinder constraint ($radius = 20\mu m$) and the case without the constraint[8] to see if there is any difference. Because of the special constraint, we limited the hit cluster size mainly to 1 and saw a perfect circle in the size-1 hit probability graph with radius about 20μm (Fig. 5).

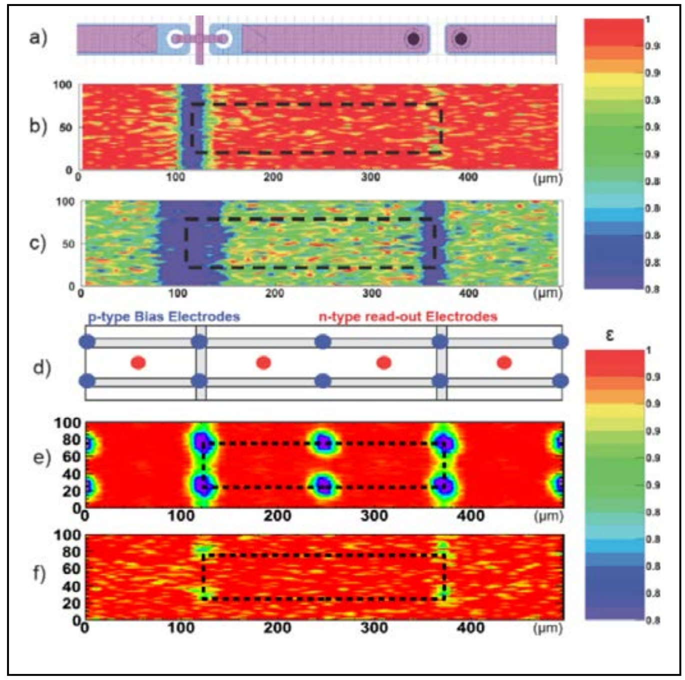

Fig. 4. Good Cell efficiency maps: a) lithography sketch for PPS, b) and c) 2D efficiency maps for PPS 61 at -1000 V (mean efficiency 96.9%) and at -600 V (mean efficiency 86.4%) using 15° inclined tracks, d) lithography sketch for 3D, e) the 2D efficiency map for the CNM 81 module using normal incident tracks (mean efficiency 97.5%) and f) the 2D efficiency map for the CNM 34 module using 15° inclined tracks (mean efficiency 99%). Both the CNM 34 and CNM81 are operated at a bias voltage of 160 V. All dimensions are in microns. See reference for details [5].

E. Varying EUDET Geometry

By varying the distance between telescope planes, i.e. Z_t in Fig. 6 and the distance between reference chip and DUT chip, i.e. Z_{d_1} & Z_{d_2}, one would be expected to observe a change of telescope resolution according to Dominik Dannheim's

[8] Actually we set the radius to be $50\mu m$, which is larger than the half diagonal length of each pixel, which is $27.5\mu m$.

calculation[9]. During our work, we calculated 40 different Z_t points equally distributed within 20 mm to 150 mm and 40 different Z_{d_1} points[10] equally distributed within 10 mm to 100 mm. Those macros and corresponding gear files for EUTelescope are generated by script EudetFileGenerator[11].

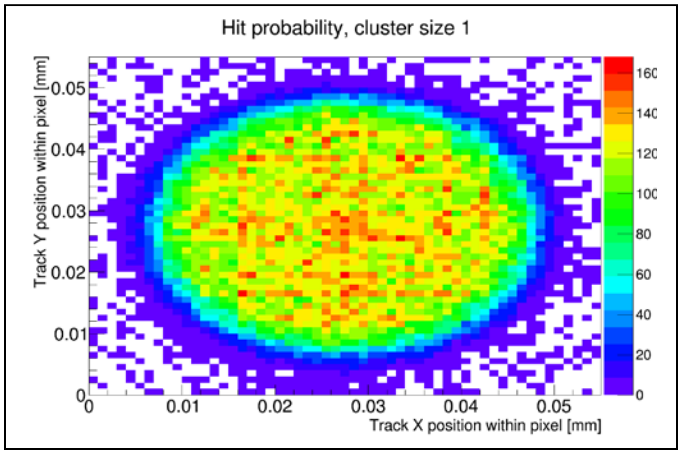

Fig. 5. Hit probablity of cluster size 1 of DESY radius = 20μm.

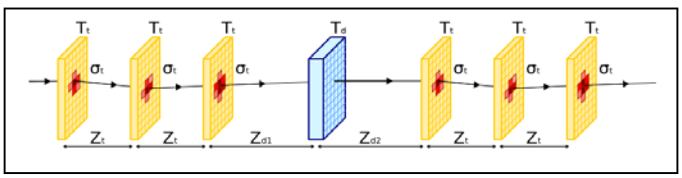

Fig. 6. Schemetic diagram for EUDET calculation.

F. *Different General Particle Source*

In order to compare the performance under different energy conditions, we adapted the particle source setup from both DESY[12], i.e. 5.6 GeV e^- particles, and CERN-SPS[13], i.e. 120~180 GeV π^- particles. The shape of the particle source are set as a rectangle in order to maximize the possibility to produce valid hits. The detailed data are displayed in Fig. 5.

```
# Source GPS rectangle
/gps/particle pi-
/gps/pos/type Plane
/gps/pos/shape Rectangle
/gps/pos/centre 0.0 0.0 -1000.0 mm
/gps/pos/halfy 5330. um
/gps/pos/halfx 5330. um
/gps/direction 0 0 1
```

Fig. 7. General Particle Source Setup in Allpix.

G. *Reconstruction Processes*

For each simulation, we calculated 400,000 events and analyzed all the data with perfect alignment files, i.e. zero shifts on the plane position, using EUTelescope v00-08-00. For the EUTelescope we computed "clusearch", "hitmaker", "fitter" steps for each simulation. For pyEudetAnalysis we computed "Reconstruction" and "Analysis" two processes. Among the output files from pyEudetAnalysis, we focused on the "resX_s1x1y1", i.e. X-residuals of 1×1 clusters and "resY_s1x1y1", i.e. Y-residuals of 1×1 clusters.

[9] Simulated plots could be found in link: http://skulis.web.cern.ch/skulis/telescope/?page=simulation

[10] Simulations were not done till this report is finished.

[11] A file generating script developed by myself. The detail usage could be found in /afs/cern.ch/work/q/qiwu/public

[12] German Electron Synchrotron A Research Centre of the Helmholtz Association. Official website: http://www.desy.de/

[13] CERN Super Proton Synchrotron. http://home.web.cern.ch/about/accelerators/super-proton-synchrotron

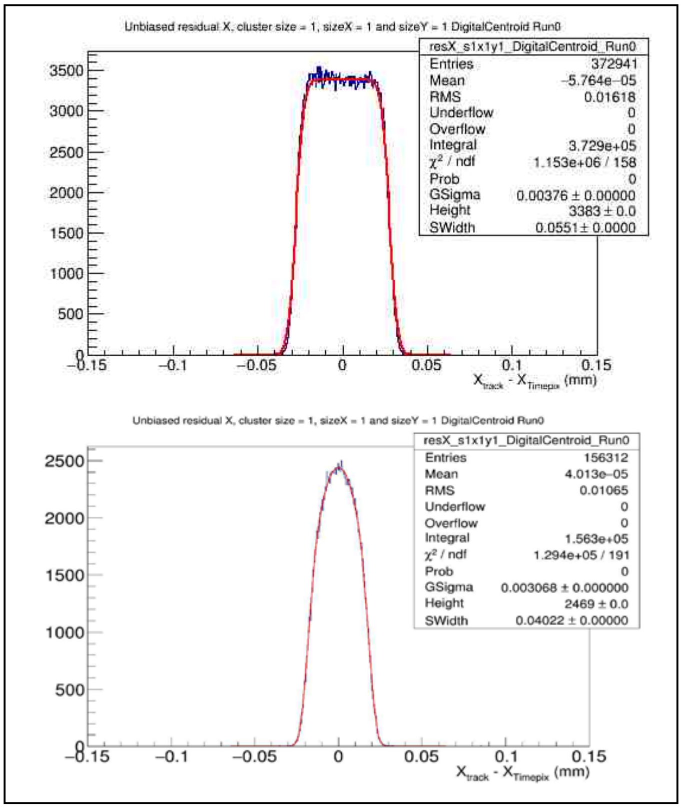

Fig. 8. X-residuals of cluster size 1 of DESY with radius = 50μm (upper) and radius = 20μm (lower).

By fitting the residuals with a modified square impulse convoluted with a Gaussian function[14], we could extract the resolution information as the value of Gaussian-Sigma. (Fig. 8) During the fitting we found that one single fitting usually could not produce well enough results, therefore we designed a Monte Carlo like algorithm to search the global minimum of the fitting parameters and avoid local minimum traps. The algorithm could be describes as following:

- ✧ Check if the first fitting failed, if true then continue, else finish the fitting
- ✧ Generate a Gaussian random vector $\vec{r}$, with mean equals to the output parameters $\overrightarrow{X_p}$ and their errors $\overrightarrow{X_e}$
- ✧ Calculate new parameter $\overrightarrow{X_p'} = \overrightarrow{X_p} + \vec{r}$ as input and run the fitting again
- ✧ Repeat from first step

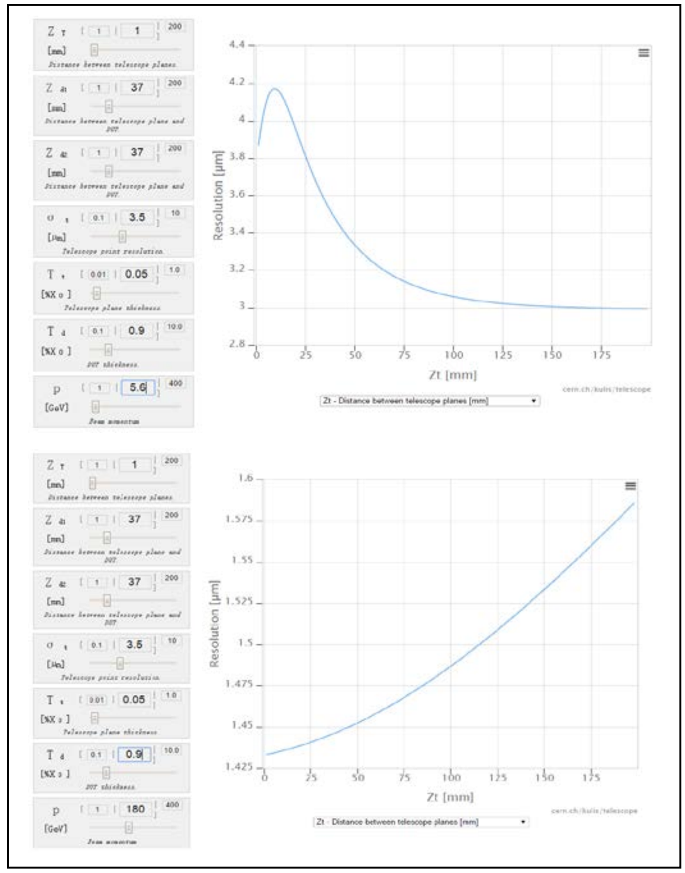

Fig. 9. Resolution calculations for DESY (upper) and SPS (lower).

III. Results

By drawing the Gaussian-Sigma with respect to Z_t, we obtained the changes of resolution under different circumstances. For low energy beam with small Z_t is (20μm~60μm), there is a

[14] For r = 20 we used $f(x, \delta, h, w, c) = \left(\frac{h\sqrt{w-(x-c)^2}}{w}\right) \otimes Gaus(x, \delta)$; for r = 50 we used $f(x, \delta, h, w, c) = Rect(x, h, w, c) \otimes Gaus(x, \delta)$

clear tendency that Gaussian sigma decreases with Z_t increasing (Fig. 12 & Fig. 10), which agreed with the theoretical calculation shown in Fig. 7; while when Z_t was large, it produced less effect on the overall telescope resolution. For SPS the relations between Gaussian sigma and Z_t was not clear from out simulation (Fig. 13 & Fig. 11), which might be caused by the inconsistence between the MIMOSA 26 digitizer used in Allpix and the SPS setup, since the MIMOSA 26 digitizer was originally designed and proofread with DESY data.

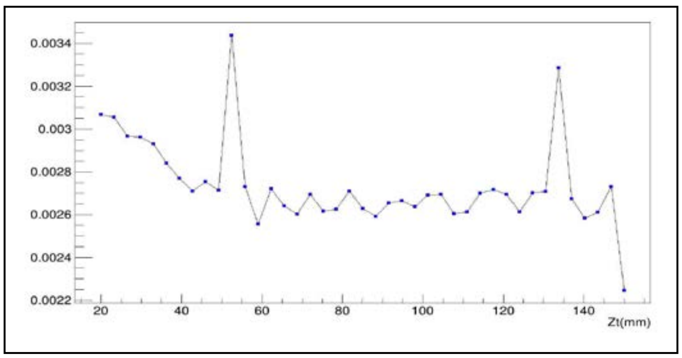

Fig. 10. GSigma-Zt plot of DESY radius = $20\mu m$.

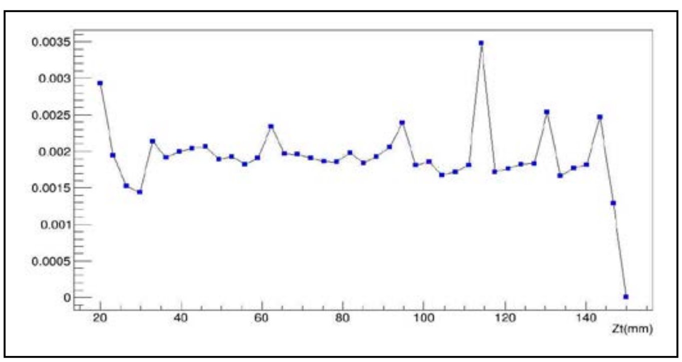

Fig. 11. GSigma-Zt plot of SPS radius = $20\mu m$.

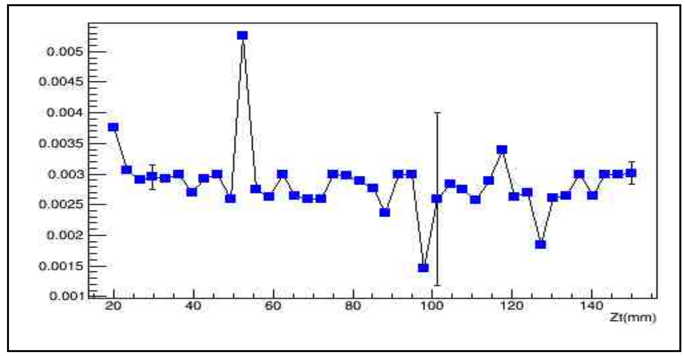

Fig. 12. GSigma-Zt plot of DESY radius = $50\mu m$.

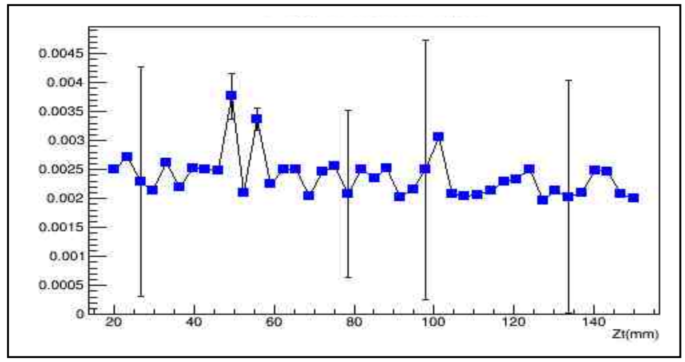

Fig. 13. GSigma-Zt plot of SPS radius = $50\mu m$.

IV. CONCLUSION

By using Allpix and EUTelescope analysis, we studied the relationship between telescope resolution and the geometric comfigurations of EUDET telescope under both high energy pion particles from SPS (180GeV) and low energy electrons from DESY (5.6GeV). By fitting the cluster-1 residuals data with a suitable function, we could be able to roughly describe and predict the hehaviors of telescope resolution under those comfigurations. By varying the distances among reference chips we found that the changing of resolution agrees with the theoretical prediction under low energy circonstances while remains unclear under high energy particles like pions.

V. ACKNOWLEDGEMENT

The authors would like to thank Mr. Mathieu Benoit, Miss Niloufar Alipour Tehrani, Mr. Francesco Armando Di Bello, Mr. Andreas Matthias Nurnberg and Miss Lingxin Meng for their helps. This work was supported in part by CERN-ATLAS, CERN-CLIC, Hong Kong University of Science and Technology and Université de Genève.

VI. Reference

[1] J. Baudot, G. Bertolone, A. Brogna, G. Claus, C. Colledani, Y. Degerli, R. D. Masi, A. Dorokhov, G. Doziere, W. Dulinski, M. Gelin, M. Goffe, A. Himmi, F. Guilloux, C. Hu-Guo, K. Jaaskelainen, M. Koziel, F. Morel, F. Orsini, M. Specht, I. Valin, G. Voutsinas and M. Winter, "First Test Results Of MIMOSA-26, A Fast CMOS," *Nuclear Science Symposium Conference Record (NSS/MIC), 2009 IEEE,* pp. 1095-7863, Oct. 24 2009-Nov. 1 2009.

[2] S. ZENZ, "Quantum Diaries," [Online]. Available: http://www.quantumdiaries.org/2008/07/25/how-a-pixel-detector-works/.

[3] M. Č. A. G. Garrin McGoldricka, "Synchronized analysis of testbeam data with the Judith software," *Nuclear Instruments and Methods in Physics Research Section A 765,* (2014) 140–145.

[4] J. B. d. M. -. U. o. Geneva, "Test-Beam Results of the AMS 180 HVCMOS prototypes," 17 Feb. 2015. [Online]. Available: https://indico.cern.ch/event/351695/session/2/contribution/48/attachments/695847/955472/JBilbaoDeMendizabal_Trento2015_SPS_TestBeamResults_HVCMOS.pdf.

[5] C. -. T. A. IBL, "Prototype ATLAS IBL Modules using the FE-I4A, http://arxiv.org/pdf/1209.1906.pdf," 10 September 2012.